Distributed Event-Triggered Model Predictive Control for Urban Traffic Lights

Wu, Na; Li, Dewei; Xi, Yugeng; De Schutter, Bart

DOI
10.1109/TITS.2020.2981381

Publication date
2021

Document Version
Final published version

Published in
IEEE Transactions on Intelligent Transportation Systems

Distributed Event-Triggered Model Predictive Control for Urban Traffic Lights

Na Wu, Dewei Li, Yugeng Xi, *Senior Member, IEEE*, and Bart de Schutter, *Fellow, IEEE*

***Abstract*— Effective traffic signal control strategies are critical for traffic management in urban traffic networks. Most existing optimization-based urban traffic control approaches update the traffic signal at regular time instants, where the length of the fixed update time interval is determined based on a trade-off between the computational efficiency and the control performance. Since event-triggered control (ETC) allows for more flexible and more efficient control than conventional time-triggered control by triggering the control action by events, and since it can refrain from redundant optimization while retaining a satisfactory behavior, we use an ETC scheme for traffic light control. In addition, based on the geographically distributed feature of traffic networks, a distributed paradigm is adopted to reduce the computational complexity for the optimization. We propose a distributed threshold-based event-triggered control strategy, where the independent triggering of agents leads to an asynchronous update of traffic signals in the system. The triggered agent then solves a mixed-integer linear programming problem and updates its traffic signals. The proposed approach is evaluated under various traffic demands by simulation, and is shown to yield the best trade-off between control performance and computational complexity compared to other control strategies.**

***Index Terms*— Distributed framework, event-triggered control, traffic signal, urban traffic congestion.**

I. Introduction

With the increasing urbanization, traffic congestion has become a major issue in modern society, especially in metropolitan areas. It not only prolongs the travel time of passengers, but also deteriorates the environment since more pollution is produced due to frequent acceleration and braking. Effective traffic signal control is one of the sustainable ways of alleviating traffic jams.

Most of the existing traffic signal strategies [1]–[5] involve time-triggered control, in which actions are determined simply by the elapse of a fixed period of time. The update of the traffic signals without consideration of real-time requirements can lead to a waste of resources with unnecessary communication and computation, especially for the uncongested regions during off-peak hours. This disadvantage can be avoided by using event-based strategies in which control actions are triggered by events rather than time.

A. Event-Triggered Control Conception

Event-triggered control (ETC), or event-based control, has received interest of a lot of researchers due to its advantages of avoiding redundant sampling and control actions. The next update of control signals in ETC is triggered by a well-defined event, which is more efficient by considering the real-time needs of systems [6]–[8]. ETC strategies possess a higher flexibility and react to external events that are not known in advance by triggering the control action only when needed. Motivated by this fact, the implementation of ETC in different types of systems has been explored [9]–[12]. An event-based proportional-integral-derivative (PID) controller has been proposed in [13] in which a new decision is made only when the error signal exceeds the threshold or the time elapsed exceeds the limit. An iterative distributed event-triggered controller has been studied for the rendezvous problem of multi-agent systems in [14]. Moreover, a model-based periodic ETC strategy has been designed in [15] in which the triggering condition is verified periodically and the information is transmitted only when needed. More studies and developments on ETC can be found in the surveys [16]–[19].

B. Event-Triggered Control in Traffic Networks

Because of the appealing advantages of ETC, several researchers have applied it in traffic systems. A traffic signal plan that switches based on the designed events has been developed in [20], where different priorities are assigned to events considering their heterogeneous importance. In addition, an event-triggered model predictive control (MPC) scheme for freeway traffic control has been developed in [21], where the ramp metering action is determined whenever the system state deviates by a certain amount from the prediction or when the elapsed time exceeds the prediction horizon. Besides, an event-triggered communication scheme for platoons has been proposed in [22] for saving communication resources.

However, few efforts have been contributed directly to the study of event-triggered control for urban traffic congestion control. The randomness and unpredictability in traffic conditions make it difficult to determine the exact update

Manuscript received August 21, 2019; revised February 17, 2020; accepted March 9, 2020. Date of publication March 23, 2020; date of current version August 9, 2021. This work was supported in part by the National Science Foundation of China under Grant 61973214, Grant 61673366, and Grant 61433002, and in part by the Science and Technology Innovation Action Plan Project of Shanghai Science and Technology Commission under Grant 18511104200. The Associate Editor for this article was S. Siri. *(Corresponding author: Bart de Schutter.)*

Na Wu, Dewei Li, and Yugeng Xi are with the Department of Automation, Shanghai Jiao Tong University, Shanghai 200240, China (e-mail: wunuo0419@sjtu.edu.cn; dwli@sjtu.edu.cn; ygxi@mail.sjtu.edu.cn).

Bart de Schutter is with the Delft Center for Systems and Control, Delft University of Technology, 2628 CD Delft, The Netherlands (e-mail: b.deschutter@tudelft.nl).

Digital Object Identifier 10.1109/TITS.2020.2981381

frequency for traffic signals at intersections. In addition, due to the heterogeneous distribution of traffic in the network, the intersections that require modifications of traffic signals may vary with the real-time traffic conditions. Even for the same region, the type of congestion also effects the congestion spread process, which results in a modification of the update frequency for the traffic signals in this region. The event-based mechanism of ETC allows for flexible changes of traffic signals according to the real-time traffic conditions.

C. Contributions and Outline

This paper contributes to the study of a traffic signal control for urban traffic networks as follows. The main contribution is that first an mixed integer linear model embedded with MPC is formulated in the distributed traffic control paradigm for each local control agent. In order to deal with the unpredictability of disturbances and the resulting vulnerability in urban traffic networks, we integrate an event-triggered mechanism into the traffic signal control strategy. In the design of the triggering conditions, we propose an evaluation method for quantifying the trend of performance in each agent under the current control strategy. Besides, the reaction time of the traffic system to the altered traffic signals is also considered to avoid oscillating control actions. Finally, the required information for the verification of the event condition in each agent, including the variables of the agent itself and of its neighbors, is provided.

The remainder of this paper is organized as follows. Sec. II presents the traffic model used for prediction and optimization and expresses it as a mixed-integer linear model. Sec. III develops the system model for each agent under the distributed MPC framework. Sec. IV describes the MILP-based distributed optimization problem of each agent, the design of the event-triggering mechanisms, and the procedure for the acquisition of the required information for both optimization and verification of event conditions in each agent. Sec. V presents a simulation-based case study and assessment of the proposed control approach for a typical network under different traffic conditions. Sec. VI summarizes the work in this paper.

II. System Model

An urban traffic network can be described by a directed graph $\mathcal{G} = (\mathcal{V}, \mathcal{E})$, where $\mathcal{V}$ denotes the set of intersections (nodes) and $\mathcal{E}$ represents the set of roads (links). The road departing from node u towards node d is indicated by an ordered pair $(u, d) \in \mathcal{E}$. The sets of input and output nodes of (u, d) are represented by $I_{u,d}$ and $O_{u,d}$ respectively. Here we use the same variable definitions as introduced in the original paper by Lin *et al.* [5]. Moreover, nodes in the network can be classified into three types: origin nodes from which exogenous vehicles enter the network, destination nodes that receive the traffic flowing outside the network, and internal nodes with signalized intersections. In this paper, the cycle split (the green time of each phase) of traffic lights at internal nodes is optimized to reduce the traffic congestion.

A. Traffic Flow Model

The distributed event-triggered MPC scheme proposed in this paper requires a traffic model for the prediction of the future behavior of the network. The developed framework allows the use of any flow model that updates the number of vehicles and outflow rate of a link at each simulation time step. In this paper, the S model proposed in [23] is selected as the prediction model.

In the S model, the number of vehicles on link (u, d) is updated by:

$$n_{u,d}(k+1) = n_{u,d}(k) + \left(\alpha^{\text{enter}}_{u,d}(k) - \alpha^{\text{leave}}_{u,d}(k)\right) \cdot T_{\text{c}} \quad (1)$$

where k is discrete time index for the traffic model and the controller, and T_{c} is the cycle length of traffic lights at each intersection and the simulation time interval. Here, T_{c} is not optimized online and is assumed to be same for all intersections. Note however, that the proposed approach can easily be extended to cases where intersections have different cycle times. The average flow rate leaving and entering link (u, d) are given by:

$$\alpha^{\text{leave}}_{u,d}(k) = \sum_{o \in O_{u,d}} \alpha^{\text{leave}}_{u,d,o}(k), \quad \alpha^{\text{enter}}_{u,d}(k) = \sum_{i \in I_{u,d}} \alpha^{\text{leave}}_{i,u,d}(k) \quad (2)$$

where

$$\begin{aligned}
\alpha^{\text{leave}}_{u,d,o}(k) &= \min\left(a_{u,d,o}(k), b_{u,d,o}(k), c_{u,d,o}(k)\right) \\
a_{u,d,o}(k) &= \beta_{u,d,o}(k) \cdot \mu_{u,d} \cdot g_{u,d,o}(k)/T_{\text{c}} \\
b_{u,d,o}(k) &= q_{u,d,o}(k)/T_{\text{c}} + \alpha^{\text{arrive}}_{u,d,o}(k) \\
c_{u,d,o}(k) &= \frac{\beta_{u,d,o}(k)}{\sum_{i \in I_{d,o}} \beta_{i,d,o}(k)} \left(C_{d,o} - n_{d,o}(k)\right)/T_{\text{c}}
\end{aligned} \quad (3)$$

The variables $a_{u,d,o}(k)$, $b_{u,d,o}(k)$, and $c_{u,d,o}(k)$ correspond to the average flow rate under saturated, unsaturated, and over-saturated traffic conditions, respectively. Moreover, $\beta_{u,d,o}(k)$ is the proportion of traffic turning from (u, d) to (d, o), which is given as an external input; $g_{u,d,o}(k)$ is the green time duration for the traffic stream leaving (u, d) towards o for time step k; $\mu_{u,d}$ is the saturated flow rate leaving (u, d); and $C_{d,o}$ is the storage capacity of link (d, o) expressed in number of vehicles.

The number of vehicles in the queue towards o is updated by

$$q_{u,d,o}(k+1) = q_{u,d,o}(k) + \left(\alpha^{\text{arrive}}_{u,d,o}(k) - \alpha^{\text{leave}}_{u,d,o}(k)\right) \cdot T_{\text{c}} \quad (4)$$

Here, $\alpha^{\text{arrive}}_{u,d,o}(k)$ is the flow rate towards o arriving at the end of queue and it is given by:

$$\begin{aligned}
\alpha^{\text{arrive}}_{u,d,o}(k) &= \beta_{u,d,o}(k) \cdot \alpha^{\text{arrive}}_{u,d}(k) \\
\alpha^{\text{arrive}}_{u,d}(k) &= \left(1 - \gamma_{u,d}(k)/T_{\text{c}}\right) \cdot \alpha^{\text{enter}}_{u,d}\left(k - \tau_{u,d}(k)\right) \\
&\quad + \gamma_{u,d}(k)/T_{\text{c}} \cdot \alpha^{\text{enter}}_{u,d}\left(k - \tau_{u,d}(k) - 1\right) \\
\phi_{u,d}(k) &= \left(C_{u,d} - q_{u,d}(k)\right) \cdot l_{\text{veh}} / \left(N^{\text{lane}}_{u,d} \cdot v^{\text{free}}_{u,d}\right) \\
\tau_{u,d}(k) &= \left\lfloor \phi_{u,d}(k)/T_{\text{c}} \right\rfloor, \ \gamma_{u,d}(k) = \phi_{u,d}(k) - \tau_{u,d}(k) \cdot T_{\text{c}}
\end{aligned} \quad (5)$$

where $\alpha^{\text{arrive}}_{u,d}(k)$ is the flow rate of vehicles arriving at the end of the queue on link (u, d); $\phi_{u,d}(k)$ is the travel time required

for a vehicle to reach the tail of the waiting queue on link (u,d) at time step k; l^{veh} is the average vehicle length; $N^{\text{lane}}_{u,d}$ is the number of lanes on link (u,d); and $v^{\text{free}}_{u,d}$ is the free flow speed of vehicles on link (u,d). Moreover, $\lfloor x \rfloor$ denotes the smallest integer not larger than x.

A more refined revision of the S model has been proposed in [24]. The control approach proposed in this paper can be easily extended to that model too.

B. Reformulation Into Mixed-Integer Linear Model

As the non-linearity of the S model will aggravate the on-line computational complexity for the optimization problem, it is reformulated as a mixed-integer linear model based on the method proposed in [5]. The leaving flow rate of each road in (3), in which the non-linearity is introduced, can be transformed into linear dynamic equations subject to linear mixed-integer inequalities, by introducing auxiliary continuous variables $z^{\text{b}}_{u,d,o}(k)$ and auxiliary binary variables $\delta^{\text{b}}_{u,d,o}(k)$.

Using the transformation and equivalences given in [5], let

$$\begin{aligned} f^{\text{b}}_{u,d,o}(k) &= b_{u,d,o}(k) - a_{u,d,o}(k) \\ f^{\text{c}}_{u,d,o}(k) &= c_{u,d,o}(k) - \min\left(a_{u,d,o}(k), b_{u,d,o}(k)\right) \end{aligned} \tag{6}$$

and define auxiliary binary variables $\delta^{\text{r}}_{u,d,o}(k)$ and auxiliary continuous variables $z^{\text{r}}_{u,d,o}(k)$ as:

$$\begin{aligned} \delta^{\text{r}}_{u,d,o}(k) &= \begin{cases} 1, & \text{if } f^{\text{r}}_{u,d,o}(k) \le 0 \\ 0, & \text{otherwise} \end{cases} \\ z^{\text{r}}_{u,d,o}(k) &= \delta^{\text{r}}_{u,d,o}(k) f^{\text{r}}_{u,d,o}(k) \end{aligned} \tag{7}$$

for $\text{r} = \text{b},\ \text{c}$. Then we have

$$\begin{aligned} \min\left(a_{u,d,o}(k), b_{u,d,o}(k)\right) &= a_{u,d,o}(k) + z^{\text{b}}_{u,d,o}(k) \\ \alpha^{\text{leave}}_{u,d,o}(k) &= a_{u,d,o}(k) + z^{\text{b}}_{u,d,o}(k) + z^{\text{c}}_{u,d,o}(k) \end{aligned} \tag{8}$$

Moreover, the statements (7) are equivalent to the following inequalities according to [5]:

$$\begin{aligned} f^{r}_{u,d,o}(k) &\le M^{r}_{u,d,o}(1 - \delta^{r}_{u,d,o}(k)) \\ f^{r}_{u,d,o}(k) &\ge \varepsilon + (m^{r}_{u,d,o} - \varepsilon)\delta^{r}_{u,d,o}(k) \\ z^{r}_{u,d,o}(k) &\le M^{r}_{u,d,o}\delta^{r}_{u,d,o}(k) \\ z^{r}_{u,d,o}(k) &\ge m^{r}_{u,d,o}\delta^{r}_{u,d,o}(k) \\ z^{r}_{u,d,o}(k) &\le f^{r}_{u,d,o}(k) - m^{r}_{u,d,o}(1 - \delta^{r}_{u,d,o}(k)) \\ z^{r}_{u,d,o}(k) &\ge f^{r}_{u,d,o}(k) - M^{r}_{u,d,o}(1 - \delta^{r}_{u,d,o}(k)) \end{aligned}$$

for $r = \text{b},\ \text{c}$, where $M^{r}_{u,d,o}$ and $m^{r}_{u,d,o}$ are the maximum and the minimum values of $f^{r}_{u,d,o}(k)$. Besides, ε is a small positive tolerance, beyond which the constraint is regarded as violated.

In addition, the entering flow rates and the arriving flow rates of links are computed based on the leaving flow rates of upstream links, which can also be formulated in a mixed-integer linear form as explained above. Thus the traffic flow model can be transformed into a mixed-integer linear (MIL) model with auxiliary binary and auxiliary continuous variables.

III. Design of the Distributed MPC Controller

Optimization-based centralized control of traffic signals in an urban traffic network can be difficult to implement in practice due to its computational complexity and its requirement for global information collection, especially in a large-scale network. On the other hand, the characteristic of transportation networks that the physically interconnected components are geographically distributed in the network is in accordance with the requirement of local information for distributed control. In this paper, we present a distributed control framework for traffic signal control, where the whole network is divided among agents in such a way that the sensing, local communication, and local decision making are handled by each agent.

Similar to [25], the whole system is described as a multi-agent system, where each agent is associated with exactly one intersection. More specifically, the area of agent i is comprised of intersection $i \in \mathcal{V}$ and its incoming links $\mathcal{E}_i = \{(j,i) | j \in \mathcal{V} \text{ and } (j,i) \in \mathcal{E}\}$, where (j,i) denotes the link from intersection j to intersection i. Then agent j is called a neighbor of agent i if there is a direct link from j to i, and the set of neighbors of agent i is denoted by $\mathcal{N}_i$. Besides, the traffic stream from link (j,i) towards intersection o is indicated by the tuple (j,i,o), and all traffic streams that flow through intersection i are denoted by $\mathcal{M}_i = \{(j,i,o) \,|\, j,o \in \mathcal{N}_i,\ \ j \neq o\}$.

A. Problem Formulation in the Distributed Set-Up

Based on the partition among agents, the numbers of vehicles and queue lengths of agent i at time step $k+1$ can be computed by:

$$n_i(k+1) = n_i(k) + T_{\text{c}} \cdot \alpha^{\text{enter}}_i(k) - T_{\text{c}} \cdot \Lambda_i \alpha^{\text{leave}}_i(k) \tag{9}$$

$$q_i(k+1) = q_i(k) + T_{\text{c}} \cdot \alpha^{\text{arrive}}_i(k) - T_{\text{c}} \cdot \Lambda_i \alpha^{\text{leave}}_i(k) \tag{10}$$

where $n_i(k),\ q_i(k),\ \alpha^{\text{enter}}_i(k),\ \alpha^{\text{arrive}}_i(k)$ are the vectors containing the corresponding variables of the links in the area of agent i, e.g., $n_i(k) = [n_{j,i}(k)]_{j \in \mathcal{N}_i}$, and $\alpha^{\text{leave}}_i(k)$ is the vector consisting of $\alpha^{\text{leave}}_{j,i,o}(k)$ of traffic stream $(j,i,o) \in \mathcal{M}_i$. Moreover, Λ_i is a selection matrix with entries 0 or 1 that maps the leaving flow rate $\alpha^{\text{leave}}_{j,i,o}(k)$ of traffic stream (j,i,o) to the leaving flow rate of link (j,i), satisfying $[\alpha^{\text{leave}}_{j,i}(k)]_{j \in \mathcal{N}_i} = \Lambda_i [\alpha^{\text{leave}}_{j,i,o}(k)]_{(j,i,o) \in \mathcal{M}_i}$.

The arriving flow rate $\alpha^{\text{arrive}}_i(k)$ for agent i is given by:

$$\alpha^{\text{arrive}}_i(k) = \tilde{B}_{i,0}(k)\alpha^{\text{enter}}_i(k) + \sum\nolimits_{t=1}^{\bar{\tau}_i(k)} \tilde{B}_{i,t}(k)\alpha^{\text{enter}}_i(k-t) \tag{11}$$

where $\bar{\tau}_i(k) = \max_{j \in \mathcal{N}_i} \tau_{j,i}(k)$ denotes the maximum of $\tau_{j,i}(k)$ of link (j,i) in the area of agent i, and $\tilde{B}_{i,0}(k)$ and $\tilde{B}_{i,t}(k)$ $(t = 1, \cdots, \bar{\tau}_i(k))$ are the coefficient matrices determined by the travel time required to reach the end of queues of roads of agent i. Let $d^{\text{q}}_i(k) = \sum_{t=1}^{\bar{\tau}_i(k)} \tilde{B}_{i,t}(k)\alpha^{\text{enter}}_i(k-t)$; then $d^{\text{q}}_i(k)$ is the arriving flow rate determined by the entering flow rate of agent i before time step k, and is treated as an input for agent i.

According to the mixed-integer linear model in Sec. II-B, let the control signals of agent i at time step k be denoted by:

$$u_i(k) = \left[g_i^T(k)\ (\delta^{\text{b}}_i(k))^T\ (\delta^{\text{c}}_i(k))^T\ (z^{\text{b}}_i(k))^T\ (z^{\text{c}}_i(k))^T \right]^T$$

where $g_i(k)$, $\delta_i^r(k)$ and $z_i^r(k)$ are the vectors consisting of $g_{j,i,o}(k)$, $\delta_{j,i,o}^r(k)$ and $z_{j,i,o}^r(k)$ respectively for all $(j,i,o) \in \mathcal{M}_i$ with $r = \mathrm{b},\ \mathrm{c}$. By suitably defining A_i, B_{ii}, B_{ji}, D_{ii}, $D_{j,i}$, E_{ji}, E_i^{c}, F_i, $K_{i,z}^r$, and $K_{i,\delta}^r$, we obtain

$$\begin{aligned} a_i(k) &= A_i u_i(k) \\ z_i^r(k) &= K_{i,z}^r u_i(k),\ \delta_i^r(k) = K_{i,\delta}^r u_i(k) \\ \alpha_i^{\mathrm{leave}}(k) &= D_{ii} u_i(k),\ \alpha_i^{\mathrm{enter}}(k) = \sum\nolimits_{j\in\mathcal{N}_i} D_{ji} u_j(k) \\ b_i(k) &= B_{ii} x_i(k) + \sum\nolimits_{j\in\mathcal{N}_i} B_{ji}(k) u_j(k) + F_i(k) d_i^{\mathrm{q}}(k) \\ c_i(k) &= \sum\nolimits_{j\in\mathcal{N}_i} E_{ji} x_j(k) + E_i^{\mathrm{c}} \end{aligned} \tag{12}$$

for $r = \mathrm{b},\ \mathrm{c}$, where $a_i(k)$, $b_i(k)$, and $c_i(k)$ are the vectorized versions of $a_{j,i,o}(k)$, $b_{j,i,o}(k)$, and $c_{j,i,o}(k)$ of traffic stream $(j,i,o) \in \mathcal{M}_i$, $F_i(k)$ involves the traffic turning rates of roads of agent i, and E_i^{c} is a vector related to the storage capacity of agent $j \in \mathcal{N}_i$. Moreover, $B_{ji}(k)$ can be computed by $B_{ji}(k) = F_i(k)\tilde{B}_{i,0}(k)D_{ji}$.

Define the state of agent i as:

$$x_i = \begin{bmatrix} n_i^T & q_i^T \end{bmatrix}^T$$

then the state equation of agent i can be given by:

$$x_i(k+1) = x_i(k) + B_{ii}^{\mathrm{s}} u_i(k) + \sum\nolimits_{j\in\mathcal{N}_i} B_{ji}^{\mathrm{s}}(k) u_j(k) + d_i^{\mathrm{s}}(k) \tag{13}$$

where $B_{ii}^{\mathrm{s}} = -T_{\mathrm{c}} \cdot [I_{|\mathcal{N}_i|}\ \ I_{|\mathcal{N}_i|}]^T \Lambda_i D_{ii}$, $B_{ji}^{\mathrm{s}} = T_{\mathrm{c}} \cdot [I_{|\mathcal{N}_i|}\ \ \tilde{B}_{i,0}^T(k)]^T D_{ji}$, and $d_i^{\mathrm{s}}(k) = T_{\mathrm{c}} \cdot [O_{|\mathcal{N}_i|}\ \ I_{|\mathcal{N}_i|}]^T d_i^{\mathrm{q}}(k)$. Moreover, 0_N and I_N represent the zero matrix and the identity matrix of dimension N, and $|\mathcal{N}_i|$ denotes the number of elements in $\mathcal{N}_i$.

On the other hand, by defining $f_i^r(k)$ as the vector consisting of $f_{j,i,o}^r(k)$ for $(j,i,o) \in \mathcal{M}_i$, $r = \mathrm{b},\ \mathrm{c}$, we have

$$\begin{aligned} f_i^{\mathrm{b}}(k) &= b_i(k) - a_i(k) \\ f_i^{\mathrm{c}}(k) &= c_i(k) - \left(a_i(k) + K_{i,z}^{\mathrm{b}} u_i(k)\right) \end{aligned}$$

Then the constraints derived from (9) for agent i can be collectively expressed as:

$$\begin{aligned} S_{ii} x_i(k) + H_{ii} u_i(k) + \sum\nolimits_{j\in\mathcal{N}_i} \left(S_{ji} x_j(k) + H_{ji} u_j(k)\right) \\ \le N_i + P_{ii} d_i^{\mathrm{q}}(k) \end{aligned} \tag{14}$$

where S_{ii}, S_{ji}, H_{ii}, H_{ji}, N_i, and P_{ii} can be derived from the given matrices and vectors. Hence, the model of agent i is denoted by the state equation (13) with constraints (14).

B. System Model Under Distributed MPC Framework

With the ability of yielding high performance by an MPC controller, a mixed-integer linear programming (MILP) problem under the MPC framework is presented in this paper, where the aforementioned S model is used as the prediction model. In this section, the model of each agent under the MPC scheme is developed

Let $\hat{\xi}_i(k) \triangleq [\hat{\xi}_i^T(k|k), \cdots, \hat{\xi}_i^T(k+N_{\mathrm{p}}-1|k)]^T$ denote the generic predicted sequence of agent i at time step k, where $\hat{\xi}_i(k+t|k)$ represents the predicted variable $\hat{\xi}_i$ for time step $k+t$ calculated at time step k, and N_{p} is the prediction horizon. Here we let $\hat{x}_i(k|k) = x_i(k)$. Without loss of generality, we assume that the prediction horizon is the same as the optimization horizon in this paper.

The predicted arriving flow rate of agent i at time step k over the prediction horizon can be given by:

$$\hat{\alpha}_i^{\mathrm{arrive}}(k) = \bar{B}_{i,0}(k)\hat{\alpha}_i^{\mathrm{enter}}(k) + \bar{B}_{i,-1}(k)\tilde{\alpha}_i^{\mathrm{enter}}(k-1) \tag{15}$$

where $\bar{B}_{i,0}(k)$ denotes the matrix that maps the predicted entering flow rate $\hat{\alpha}_i^{\mathrm{enter}}(k)$ to the predicted arriving flow rate $\hat{\alpha}_i^{\mathrm{arrive}}(k)$, $\bar{B}_{i,-1}(k)$ denotes the matrix that relates $\hat{\alpha}_i^{\mathrm{arrive}}(k)$ to $\tilde{\alpha}_i^{\mathrm{enter}}(k-1) = [(\alpha_i^{\mathrm{enter}}(k-\bar{\tau}_i(k)))^T, \cdots, (\alpha_i^{\mathrm{enter}}(k-1))^T]^T$, which collects the required entering flow rate of agent i before time step k. Here, $\bar{d}_i^{\mathrm{q}}(k) = \bar{B}_{i,-1}(k)\tilde{\alpha}_i^{\mathrm{enter}}(k-1)$ is treated as an input for agent i.

Then we can get the state equation of agent i under the MPC scheme:

$$\hat{x}_i(k) = \bar{A}_i^{\mathrm{s}} x_i(k) + \bar{B}_{ii}^{\mathrm{s}} \hat{u}_i(k) + \sum\nolimits_{j\in\mathcal{N}_i} \bar{B}_{ji}^{\mathrm{s}}(k)\hat{u}_j(k) + \bar{d}_i^{\mathrm{s}}(k) \tag{16}$$

where $\bar{A}_i^{\mathrm{s}} = [I_{2|\mathcal{N}_i|}, \cdots, I_{2|\mathcal{N}_i|}]^T$, $\bar{B}_{ii}^{\mathrm{s}} = L_{N_{\mathrm{p}}} \otimes B_{ii}^s$, $L_{N_{\mathrm{p}}}$ is a lower triangular matrix of dimension N_{p} with all the entries below the main diagonal equal to 1, and with $\otimes$ denoting the Kronecker product. Moreover, $\bar{B}_{ji}^{\mathrm{s}}(k) = T_{\mathrm{c}} \cdot (L_{N_{\mathrm{p}}} \otimes [I_{|\mathcal{N}_i|}\ \ O_{|\mathcal{N}_i|}]^T + (L_{N_{\mathrm{p}}} \otimes [O_{|\mathcal{N}_i|}\ \ I_{|\mathcal{N}_i|}]^T)\bar{B}_{i,0}(k)) \cdot \bar{D}_{ji}$, $\bar{D}_{ji} = I_{N_{\mathrm{p}}} \otimes D_{ji}$, $\bar{d}_i^{\mathrm{s}}(k) = (L_{N_{\mathrm{p}}} \otimes [O_{|\mathcal{N}_i|}\ \ I_{|\mathcal{N}_i|}]^T) \cdot \bar{d}_i^{\mathrm{q}}(k)$.

On the other hand, the constraints in (14) under the MPC framework can be written as:

$$\begin{aligned} &\bar{S}_{ii}\hat{x}_i(k) + \bar{H}_{ii}\hat{u}_i(k) \\ &\quad + \sum\nolimits_{j\in\mathcal{N}_i} \left(\bar{S}_{ji}\hat{x}_j(k) + \bar{H}_{ji}\hat{u}_j(k)\right) \le \bar{N}_i + \bar{P}_{ii}\bar{d}_i^{\mathrm{q}}(k) \end{aligned} \tag{17}$$

where $\bar{X} = I_{N_{\mathrm{p}}} \otimes X$ for $X \in \{S_{ii}, S_{ji}, H_{ii}, H_{ji}, P_{ii}\}$, $\bar{N}_i = e_{N_{\mathrm{p}}} \otimes N_i$, and $e_{N_{\mathrm{p}}}$ is an unit column vector of dimension N_{p}. Therefore, the model of agent i under MPC framework is represented by (16) with constraints of (17).

IV. Distributed Event-Triggered Traffic Control Optimization

We propose a distributed event-triggered MPC scheme for traffic signal control, where agents work in parallel and the independent triggering mechanism of each agent leads to an asynchronous update of control signals in the system, which makes the proposed distributed ETC approach more flexible than the centralized ETC strategies where all agents are triggered at the same time. The optimization problem in each agent is formulated as follows.

A. MILP-Based Distributed MPC for the Traffic Network

In this paper, the total time spent (TTS) of vehicles in the network over the optimization time intervals is selected as the objective function:

$$J_{\mathrm{tot}}(k) = \sum\nolimits_{t=1}^{N_{\mathrm{p}}} \sum\nolimits_{(u,d)\in\mathcal{E}} T_{\mathrm{c}} \cdot \hat{n}_{u,d}(k+t|k)$$

which can be separable across agents by $J_{\text{tot}}(k) = \sum_{i\in\mathcal{V}} J_i(k)$, where

$$J_i(k) = \sum\nolimits_{t=1}^{N_\text{p}} \sum\nolimits_{j\in\mathcal{N}_i} T_\text{c} \cdot \hat{n}_{j,i}(k+t|k) \tag{18}$$

Note however, that the proposed approach also works for other objective functions that indicate the network performance, such as the average speed of vehicles and the total delay time.

Then the optimization problem of agent i can be formulated as follows:

$$\begin{aligned} P_i(k): \min\nolimits_{\hat{u}_i(k)} \hat{J}_i(k) &= p_i^T \hat{x}_i(k+1) \\ \text{s.t. } & (16)-(17) \\ & \hat{u}_i(k+t|k) \in \mathcal{U}_i,\ \hat{x}_i(k+t+1|k) \in \mathcal{X}_i \\ & \text{for } t = 0,\ \cdots,\ N_\text{p}-1 \end{aligned} \tag{19}$$

where p_i is a suitably defined vector, and $\mathcal{U}_i(k)$ and $\mathcal{X}_i(k)$ denote the feasible sets of control signals and states of agent i, which can be easily formulated as linear equalities and inequalities. Hence, with a linear objective function and mixed-integer linear constraints, the optimization problem can be formulated as an MILP problem. The solution of the optimization is denoted by $\hat{u}_i^*(k) = [(\hat{u}_i^*(k|k))^T, \cdots, (\hat{u}_i^*(k+N_\text{p}-1|k))^T]^T$, and the corresponding optimal state trajectory and objective function are denoted by $\hat{x}_i^*(k)$ and $J_i^*(k)$, respectively.

At each time step, to determine whether the current traffic signal settings are suitable, the predicted TTS of vehicles $\bar{J}_i(k)$ of each agent $i \in \mathcal{V}$ over the prediction horizon is evaluated under a feasible control scheme $\bar{u}_i(k) = [\bar{u}_i^T(k|k), \cdots, \bar{u}_i^T(k+N_\text{p}-1|k)]^T$ in this paper. Before introducing the event triggering conditions, the construction method for a feasible control sequence is given as follows.

B. The Feasible Control Trajectory

Let $\{k_m^i\}_{m\in\mathbb{N}} = k_0^i, k_1^i, \cdots$ denote the triggered time steps for agent $i \in \mathcal{V}$, where $k_{m-1}^i < k_m^i < k_{m+1}^i$ and $k_m^i \in \mathbb{N}$. We assume that the latest triggered time step of agent i before time step k is k_m^i, i.e., $k_m^i < k < k_{m+1}^i$. Then let

$$\bar{\xi}_i(k) = \left[\bar{\xi}_i^T(k|k), \ldots, \bar{\xi}_i^T(k|k+N_\text{p}-1)\right]^T$$

denote the feasible sequence of ξ_i over the optimization horizon at time step k.

First, the feasible traffic signal $\bar{g}_i(k)$ of agent i is constructed based on the optimal traffic signal $\hat{g}_i^*(k_m^i)$ obtained at time step k_m^i:

$$\bar{g}_i(k+t|k) \triangleq \begin{cases} \hat{g}_i^*(k+t|k_m^i), & t = 0, \cdots, (k_m^i+N_\text{p}-1)-k \\ \hat{g}_i^*(k_m^i+N_\text{p}-1|k_m^i), & t = (k_m^i+N_\text{p})-k, \cdots, N_\text{p}-1 \end{cases}$$

The relation between $\hat{g}_i^*(k_m^i)$ and $\bar{g}_i(k)$ is indicated in Fig. 1. Then $\bar{u}_i(k)$ and $\bar{J}_i(k)$ can be obtained by the following steps:

1) Initialization: let $t = 0$ and set $\bar{x}_i(k|k) = x_i(k)$.

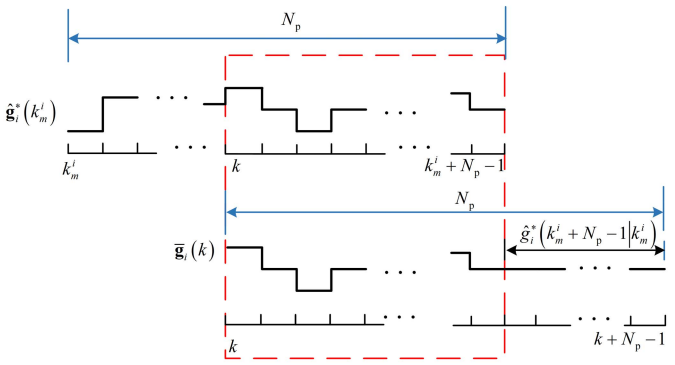

Fig. 1. The relation between the optimal control trajectory $\hat{g}_i^*(k_m^i)$ and the feasible control trajectory $\bar{g}_i(k)$ of agent i at time step k.

2) Compute $\bar{a}_i(k+t|k)$, $\bar{b}_i(k+t|k)$, and $\bar{c}_i(k+t|k)$ based on (3) and (12):

$$\begin{aligned} \bar{a}_i(k+t|k) &= A_i^g \bar{g}_i(k+t|k) \\ \bar{b}_i(k+t|k) &= B_{ii}\bar{x}_i(k+t|k) + \hat{\alpha}_i^{\text{arrive}}(k+t|k) \\ \bar{c}_i(k+t|k) &= \sum\nolimits_{j\in\mathcal{N}_i} E_{ji}\hat{x}_j(k+t|k) + E_i^\text{c} \\ \hat{\alpha}_i^{\text{arrive}}(k+t|k) &= \sum_{j\in\mathcal{N}_i}\sum_{h=0}^{\bar{\tau}_i(k)} B_{ji,h}(k)\hat{u}_j(k+t-h|k) \end{aligned}$$

where A_i^g and $B_{ji,h}(k)$ are appropriately defined matrices.

3) Compute $\bar{z}_i^r(k+t|k)$ and $\bar{\delta}_i^r(k+t|k)$ (for $r = \text{b},\ \text{c}$) according to (6) and (7).
4) Compute the feasible control signal $\bar{u}_i(k+t|k)$ with $\bar{g}_i(k+t|k)$, $\bar{\delta}_i^r(k+t|k)$, and $\bar{z}_i^r(k+t|k)$ (for $r = \text{b},\ \text{c}$), and compute the corresponding feasible state $\bar{x}_i(k+t+1|k)$ according to (13).
5) If $t < N_\text{p}-1$, let $t := t+1$ and go to step 2); otherwise go to step 6).
6) Compute $\bar{J}_i(k)$ according to (19) and exit.

From step 1) to 6), given the optimal traffic signal $\hat{g}_i^*(k_m^i)$ of agent i at the last triggered time step k_m^i, the current state $x_i(k)$ at time k, and the information $\hat{x}_j(k)$ and and $\hat{u}_j(k)$ from agents $j \in \mathcal{N}_i$, the feasible control trajectory $\bar{u}_i(k)$, the corresponding feasible state $\bar{x}_i(k)$ and objective function $\bar{J}_i(k)$ of agent i under $\bar{u}_i(k)$ can be obtained.

C. Information Exchange Among Neighbors

From the analysis above, whether to solve the optimization problem denoted by $P_i(k)$, or to construct the feasible control sequence $\bar{u}_i(k)$ of agent i, variables including $\hat{x}_j(k)$ and $\hat{u}_j(k)$ from the neighboring agents $j \in \mathcal{N}_i$ are required, where $\hat{u}_j(k) = [\hat{u}_j^T(k|k)\ \cdots\ \hat{u}_j^T(k+N_\text{p}-1|k)]^T$. According to the mechanisms of the distributed event-triggered control scheme, the neighboring agent j transmits its updated information to i only at its triggered time steps.

Let $k_{m'(k)}^j$ denote the last triggered time step of agent j before k, and $\tilde{x}_j(k_{m'(k)}^j)$ and $\tilde{u}_j(k_{m'(k)}^j)$ denote the transmitted states and the transmitted control signals of agent j to i at time step $k_{m'(k)}^j$. If the variables $\hat{u}_j(k)$ and $\hat{x}_j(k)$ are included

in the transmitted $\tilde{u}_j(k^j_{m'(k)})$ and $\tilde{x}_j(k^j_{m'(k)})$, then they can be directly used in the optimization of $P_i(k)$ and the construction of $\bar{u}_i(k)$ of agent i.

Since the time intervals between two consecutive triggered time steps of each agent is less then the prediction horizon N_p, we have

$$k - k^j_{m'(k)} \le N_\mathrm{p},\ k + N_\mathrm{p} - 1 \le k^j_{m'(k)} + 2N_\mathrm{p} - 1$$

Let the transmitted information

$$\tilde{\xi}_j(k^j_{m'(k)}) = [\tilde{\xi}^T_j(k^j_{m'(k)}|k^j_{m'(k)}), \cdots,\ \tilde{\xi}^T_j(k^j_{m'(k)} + 2N_\mathrm{p} - 1|k^j_{m'(k)})]^T$$

with $\tilde{\xi}_j \in \{\tilde{x}_j, \tilde{u}_j\}$; then the predicted variables of $\hat{x}_j(k)$ and $\hat{u}_j(k)$ can be obtained by letting $\hat{x}_j(k+t|k) = \hat{x}_j(k+t|k^j_{m'(k)})$, and $\hat{u}_j(k+t|k) = \hat{u}_j(k+t|k^j_{m'(k)})$

On the other hand, at time step $k^j_{m'(k)}$, the optimal control sequence $\hat{u}^*_j(k^j_{m'(k)})$ and the optimal state trajectory $\hat{x}^*_j(k^j_{m'(k)})$ of agent j are obtained after solving its optimization problem, which involve the predicted variables $\hat{u}^*_j(k^j_{m'(k)}+t|k^j_{m'(k)})$ and $\hat{x}^*_j(k^j_{m'(k)}+t|k^j_{m'(k)})$ for $t = 0, \ldots, N_\mathrm{p}-1$. The predicted values of $\tilde{u}_j(k^j_{m'(k)}+t|k^j_{m'(k)})$ and $\tilde{x}_j(k^j_{m'(k)}+t|k^j_{m'(k)})$ for $t = N_\mathrm{p}, \ldots, 2N_\mathrm{p}-1$ can be obtained by letting $\tilde{g}_j(k^j_{m'(k)}+t|k^j_{m'(k)}) = \hat{g}^*_j(k^j_{m'(k)}+N_\mathrm{p}-1|k^i_m)$ for $t = N_\mathrm{p}, \ldots, 2N_\mathrm{p}-1$ and following the construction steps in Sec. IV-B. Noted that other methods such as time series forecasting or neural network models [26]–[28] that can provide $\tilde{x}_j(k^j_{m'(k)})$ and $\tilde{u}_j(k^j_{m'(k)})$ can also be used.

D. Event-Triggering Mechanism

In Sec. IV-B, the objective function $\bar{J}_i(k)$ of agent $i \in \mathcal{V}$ is computed based on the updated state $x_i(k)$ and the constructed feasible control sequence $\bar{u}_i(k)$ at time step k. With $x_i(k)$ a reflection of the effect of $\hat{u}^*_i(k^i_m)$ from time step k^i_m to k and the effect of the traffic condition, and $\bar{u}_i(k)$ constructed based on $\hat{u}^*_i(k^i_m)$ and $x_i(k)$, $\bar{J}_i(k)$ provides an insight of the effects of $\hat{u}^*_i(k^i_m)$ on the TTS of agent i under the current traffic situation. Thus the increment of the predicted TTS $\bar{J}_i(k)$ compared with $J^*_i(k)$ of each agent is viewed as an indication of performance deterioration under the current control scheme.

For agent i, the error between $\bar{J}_i(k)$ and the optimal objective value $J^*_i(k^i_m)$ is computed at time steps $k = k^i_m+1,\ k^i_m+2, \cdots, k^i_{m+1}-1$. When the error exceeds the given threshold, it implies that the predicted travel time spent by vehicles will be prolonged, and $\hat{u}^*_i(k^i_m)$ is not appropriate anymore under the current traffic situation. Thus the first event condition that triggers the update of traffic signals for each agent $i \in \mathcal{V}$ is defined as:

$$\mathcal{C}^i_1(k) = \begin{cases} 1, & \text{if } \bar{J}_i(k) - J^*_i(k^i_m) > \varepsilon^i_1 \\ 0, & \text{otherwise} \end{cases} \tag{20}$$

where ε^i_1 is a positive threshold that corresponds to the TTS deviation. It is determined by the tolerance of the traffic system to bad control signals, and is thus determined by considering the trade-off between the control performance and the use of communication resources. Moreover, we use the boolean variable $\mathcal{C}^i_1(k)$ with 1 representing that the corresponding statement "true" and 0 representing "false". The trade-off between the triggering frequency of agent i and the performance of its controller can be adjusted through ε^i_1.

On the other hand, it takes a period of time for the traffic system to respond to the updated traffic signals, similar to the rising time of a linear time-invariant system in the step response. Thus a *minimum* inter-event time for the execution of the optimized control scheme is imposed on each agent $i \in \mathcal{V}$ to avoid the triggering resulting from insufficient execution time. Thus the second triggering condition is defined as:

$$\mathcal{C}^i_2(k) = \begin{cases} 1, & \text{if } k - k^i_m \ge \varepsilon^i_2 \\ 0, & \text{otherwise} \end{cases} \tag{21}$$

where $\varepsilon^i_2 \in \mathbb{N}$ is a positive threshold and corresponds to the minimum inter-event time. It is determined by the average time it takes for the improvement of the control performance to begin to appear under the updated control signals.

Moreover, the traffic signals of each agent $i \in \mathcal{V}$ will be updated when the whole control sequence optimized at last triggered time step has been implemented completely. Then the third event condition is defined as:

$$\mathcal{C}^i_3(k) = \begin{cases} 1, & k - k^i_m = N_\mathrm{p} \\ 0, & k - k^i_m < N_\mathrm{p} \end{cases} \tag{22}$$

The third event condition corresponds to the prediction horizon N_p, and is determined by the average journey time of the vehicles in the network.

The three pre-defined thresholds are related to the control objectives and the characteristics of the traffic system, and are thus fixed in our paper. Here we just provide one of the possible triggering mechanisms for the application of the event-triggered control in urban traffic networks. Other factors such as the road grades, the congestion distribution in the network, the triggering conditions of neighboring areas, and so on can also be considered in the triggering mechanisms. The corresponding thresholds can be designed fixed or dynamical according to the specific event conditions, the physical constraints, the control objectives of the system, and so on, which can be investigated in our future research.

Let $\mathcal{C}^i$ denote the triggering rule of agent i that determines the computation of a new control sequence; then the traffic signal of agent i will be updated when

$$\mathcal{C}^i(k) = 1, \quad \text{with } \mathcal{C}^i(k) = \left(\mathcal{C}^i_1(k) \wedge \mathcal{C}^i_2(k)\right) \vee \mathcal{C}^i_3(k) \tag{23}$$

where $\wedge$ denotes the logical operator "AND", and $\vee$ denotes the logical operator "OR". The event condition in (23) will be checked at each time step by each agent $i \in \mathcal{V}$, and the event times are defined by $\mathcal{C}^i(k^i_m) = 1$, for $m = 0, 1, \cdots$.

Above all, in the distributed event-triggered control scheme, the control law of each agent is updated by solving the MILP problem denoted by $P_i(k)$ based on the real-time information of the agent and the transmitted information from neighboring agents at their last triggered time steps only when the agent is triggered. Then the transmitted information of the triggered

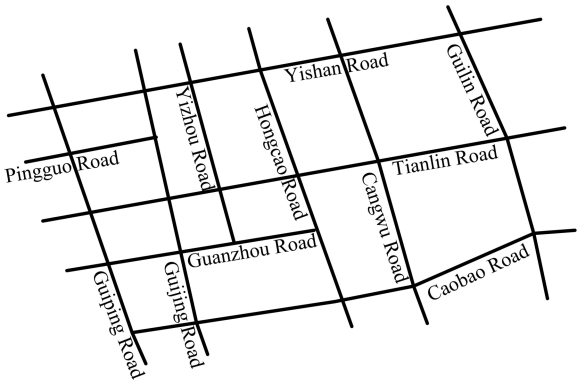

Fig. 2. The geometry of an area within the Caohejing district in Shanghai.

agent to its neighbors is constructed according to the above procedures. The obtained optimal control sequence will be implemented until next the triggered time step. At each time step, the feasible control sequence of each agent is constructed according to the procedures in Sec. IV-B for the verification of the triggering conditions in the agent.

In the distributed paradigm, only local information is used in the independent optimization of the traffic signals in each agent. The associated variables among agents are predicted by each agent at its own triggered time steps and transmitted to the neighbors. Thus the proposed distributed control scheme only provides suboptimal solutions.

V. Case Study

To evaluate the effectiveness of the proposed distributed event-triggered control (DETC) approach, we assess its performance by comparing it with various existing control approaches. The simulation is carried out by the open source microscopic road traffic simulation package SUMO ("Simulation of Urban MObility") [29] to emulate the real traffic environment. All the optimization problems are solved in the Matlab 2017 environment on a computer with a 3.5-GHz Intel Xeon Processor E5 and 32GB of RAM.

A. Road Network and Setup

The road network in Fig. 2 is based on an area within the Caohejing district in Shanghai, China. It consists of 41 nodes including 23 internal intersections controlled by traffic lights and 18 simultaneous origin and destination nodes for generating and absorbing traffic, and 53 two-way roads ranging from 110 m to 618 m. The specific parameters for each road can be found in Google Maps by searching their names. The lower and upper bounds of the green time in each phase are 10 s and 50 s, and the cycle time T_c is 80 s for all intersections. In addition, the prediction horizon N_p is set to 10, which is sufficient for guaranteeing the short-term performance while resulting in a reasonable computational burden. The threshold in the second event condition is $\varepsilon_2 = 3$ for all agents.

We have run simulations in SUMO and applied system identification on the resulting data to determine the parameters of the S model, which gives the following values: the saturated flow rate of vehicles $\mu = 1.2$ veh/s, the average vehicle length $l_{\text{veh}} = 6.5$ m, and the free flow speed $v_{\text{free}} = 7.8$ m/s. Here we assume the same values for each of the links. As we have run abundant simulations in the identification process with various traffic conditions, these values are adequate approximations for parameters of the traffic model.

The network is lightly loaded at the start of the simulation. The simulation will not be terminated until all the vehicles have arrived at their destinations. Thus the simulation time is different for the control strategies due to their different control performance.

B. Compared Schemes

In the simulation, the performance of the proposed DETC is evaluated against the following control approaches:

- simplified SCOOT [30], a traffic responsive control strategy.
- DATTC, under which the traffic lights of intersections are updated at regular time intervals. The update frequency of each intersection is equal to the average triggering frequency of the corresponding intersection controlled by DETC.
- Distributed time-triggered control (DTTC), under which the traffic signals of each intersection are updated at each time step.
- Centralized event-triggered control (CETC), a centralized control strategy that updates the traffic signals of all intersections when triggered. The triggering rule is the same as that of DETC, but with the first triggering condition replaced by the increment of the predicted TTS of all intersections.

The implementation of SCOOT is based on [30] which is publicly available in the literature and describes a simplified version of SCOOT. In this paper, only a split optimizer is implemented, while the offset between intersections and the cycle times are fixed during the simulation. Before the end of each phase, the split optimizer determines whether to anticipate the start of the next phase, as scheduled, or to delay it by minimizing the estimated sum of queue lengths on the incoming links based on the data from detectors placed at the entrance of the approaches. The corresponding decisions are made by the split optimizers of each intersection independently. Thereby, the alteration of the green time duration is at most 4 seconds each time. In addition, in the proposed distributed control scheme, the green time duration of each phase is constrained between the same lower and upper bounds.

C. Measurements of Effectiveness

In order to measure the control performance of different strategies, the following criteria are compared in the simulation:

- traffic queue length, i.e. the total number of vehicles in the network with speed less than 0.1 m/s.
- network throughput, which is defined as the accumulated number of vehicles that have arrived at their destinations so far.

- TTS, the accumulated TTS of all the vehicles since the beginning of the simulation.
- optimization CPU time, where t_{ave} is the average optimization CPU time, and $t_{\max}$ is the maximum optimization CPU time of the worst case during the simulation.
- the average triggering rate, which is the ratio of the number of triggered time steps over the total number of simulation time steps. A higher triggering rate of control schemes will result in a larger computation and communication burden.

D. Computational Complexity

In the optimization of traffic signals in each intersection $i \in \mathcal{V}$, 2 integer and 2 continuous variables in (7) and 12 constraints represented by (9) are introduced to compute the leaving flow rate of each traffic stream $(j, i, o) \in \mathcal{M}_i$. On the other hand, three or two continuous variables are introduced for representing the green time of the traffic signals in each intersection. For a 4-arm intersection with 4 phases, there are $4 \times 3 = 12$ traffic streams with each link having 3 downstream links. Therefore, there are $2 \times 12 + 3 = 27$ continuous variables, $2 \times 12 = 24$ integer variables, and $12 \times 3 \times 4 = 144$ mixed-integer linear constraints in the optimization problem of the intersection. Similarly, for a 3-arm intersection with 3 phases, there are $3 \times 3 = 9$ traffic streams. Therefore, there are $2 \times 9 + 2 = 20$ continuous variables, $2 \times 9 = 18$ integer variables, and $12 \times 3 \times 3 = 108$ mixed-integer linear constraints in the optimization problem of the intersection.

For the distributed controller (DETC, DTTC, and DATTC) with the prediction horizon $N_{\text{p}} = 10$, the number of the continuous and the integer variables, and the number of the mixed-integer linear constraints will be ten times in each agent. For the centralized controller (CETC) with $N_{\text{p}} = 10$, since there are nineteen 4-arm intersections and four 3-arm intersections in the network, the optimization problem will involve $(27 \times 19 + 20 \times 4) \times 10 = 5930$ continuous variables, $(24 \times 19 + 18 \times 4) \times 10 = 5280$ integer variables, and $(144 \times 19 + 108 \times 4) \times 10 = 31680$ mixed-integer linear constraints.

Because of the large number of optimization variables and constraints involved in CETC, we limit the time of each optimization in the CETC scheme by an upper bound of 3600 s, which is sufficiently large for it. Additional experiments not reported here have shown that longer computation times only bring very small performance improvements. Note however, that in fact a control scheme with 3600 s of optimization time is not realistic for real-time implementation. So here we use CETC as a benchmark for measuring the degradation of control performance and the improvement of CPU time of DETC compared to a centralized scheme.

E. Simulation Results

In the simulation, vehicles are inserted into the network during the first 90 cycles where each cycle takes 80 s, and the origin and the destination of vehicles are randomly selected from 18 external nodes. The control performance of the proposed control strategy is evaluated under 3 scenarios from low traffic demands (Scenario 1) to heavy traffic demands (Scenario 3) as shown in Table I.

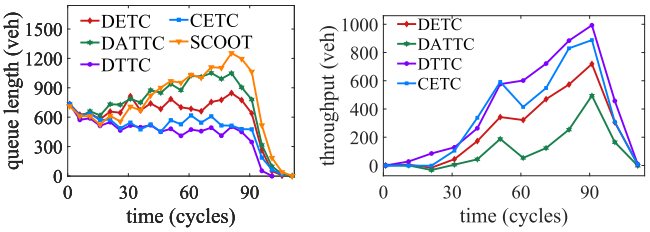

(a) Queue length for Scenario 1 (b) Relative throughput for Scenario 1

Fig. 3. Simulation results for Scenario 1.

Due to the event conditions of (21) and (22) in Sec. IV-D, the triggering rate of each intersection in the event-triggered schemes DETC and CETC falls between $1/N_{\text{p}}$ and $1/\varepsilon_2^i$. Moreover, as the simplified SCOOT determines whether to adjust the green time before each phase, it is triggered 3 times in each cycle for a 4-phase signalized intersection and 2 times for a 3-phase intersection considering the cycle time constraint. Thus the average triggering rate of SCOOT is the average value over all intersections in the network: $(3 \times 19 + 2 \times 4) \div 23 = 2.83$. As for DTTC, considering that the traffic signals for each agent are updated at each time step, its triggering rate is 1.

1) Scenario 1: The proposed control strategy is evaluated under the light traffic congestion with a low traffic demand.

In Table I, the maximum queue length during the simulation is reduced from 1289 vehicles under the simplified SCOOT scheme to 850 vehicles under DETC, and it is further reduced to 733 vehicles by DTTC and CETC. Besides, the queue length under DETC fluctuates within 600-850 vehicles before the 90th time step, whereas it is decreased since the beginning of the simulation and is maintained below 700 vehicles under DTTC and CETC in Fig. 3(a). Moreover, because each agent in the distributed control strategy solves a optimization problem with less variables and constraints, the average CPU time is significantly reduced by about 4 orders of magnitudes in the DETC scheme compared with CETC. In addition, the maximum CPU time is 1.54 s under DETC, which is much less than 85.4 s under DTTC. In addition, the average triggering rate of CETC is 0.31, which is very close to the maximum triggering rate 0.33. It reveals a high update frequency of CETC even under light traffic congestion. Since CETC focuses on the overall traffic condition, the update of traffic signals will be triggered by the deterioration of the traffic condition in any area in the network. In contrast, the average triggering rate of DETC and DATTC is 0.13, only half of that under CETC.

The relative throughput of the network computed as the difference between the throughput of each control scheme and that of the simplified SCOOT scheme is shown in Fig. 3(b). It shows that with the light traffic demand, the throughput of the DETC, the DTTC, and the CETC scheme is comparable. The maximum difference of the throughput between the DETC and the DTTC scheme is 332 vehicles, which is about 2.3% of the total throughput.

2) Scenario 2: Under the medium traffic demand, the performance of the simplified SCOOT scheme degrades

TABLE I

SUMMARY OF THE SIMULATION RESULTS

Scenario	time steps	traffic demand (veh·h)	strategy	$q_{\max}$ (veh)	TTS ($\times 10^3$ veh·h)	improvement of the TTS with respect to SCOOT (%)	t_{ave} (s)	$t_{\max}$ (s)	average triggering rate
Scenario 1	1-30	225	DETC	850	1.74	18.8	0.23	1.54	0.13
			DATTC	1142	2.06	3.9	0.26	2.68	0.13
	31-60	240	DTTC	733	1.28	40.7	0.91	85.4	1
			CETC	733	1.42	33.6	3579	3743	0.31
	61-90	135	SCOOT	1289	2.14	-	0.03	0.05	2.83
Scenario 2	1-90	600	DETC	1552	2.92	76.4	0.41	4.94	0.18
			DATTC	2579	4.50	63.7	0.52	5.43	0.18
			DTTC	940	1.82	85.3	1.36	105.17	1
			CETC	1189	2.08	83.3	3626	3828	0.31
			SCOOT	3728	12.40	-	0.07	0.12	2.83
Scenario 3	1-90	700	DETC	2860	6.40	75.4	1.11	7.11	0.21
			DATTC	2536	5.96	77.1	0.88	10.26	0.21
			DTTC	1736	4.01	84.6	3.72	212.68	1
			CETC	2066	4.66	82.1	3622	3846	0.31
			SCOOT	4105	26.04	-	0.06	0.38	2.83

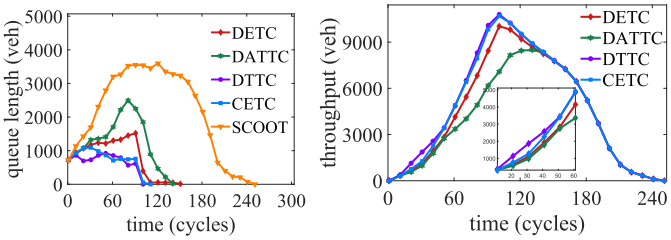

(a) Queue length for Scenario 2 (b) Relative throughput for Scenario 2

Fig. 4. Simulation results for Scenario 2.

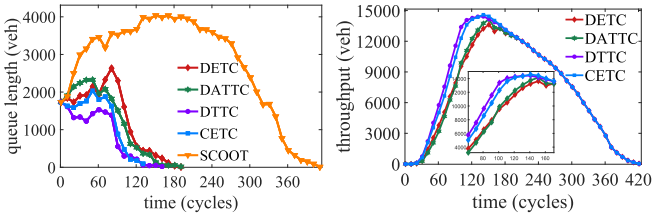

(a) Queue length for Scenario 3 (b) Relative throughput for Scenario 3

Fig. 5. Simulation results for Scenario 3.

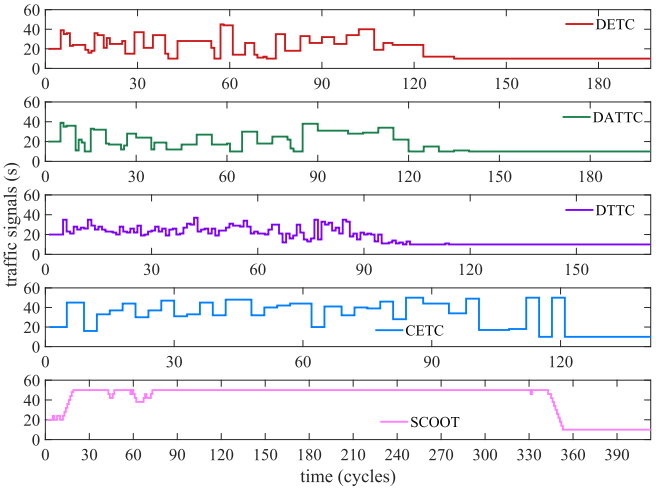

Fig. 6. Traffic signals for the selected representative intersection under different control strategies.

significantly compared with the other schemes, implied by the large gap in the criteria such as traffic queue length, TTS, and the throughput. The TTS under the simplified SCOOT can be reduced by more than 75% under DETC, CETC, and DTTC, as shown in Table I. Although the optimization CPU time of all strategies is increased compared to Scenario 1, the maximum CPU time under DETC is 4.9 s, which is negligible compared to 105.1 s under DTTC and 3828 s under CETC. Besides, the average triggering rate of DETC is 0.18, which is still much lower than 0.31 under CETC.

The queue length and the relative throughput of the network are given in Fig. 4. Since the 60th time step, the queue length under DATTC begins to diverge with that under DETC, which is also the time instant from which the relative throughput of DATTC begins to deviate from that of DETC in Fig. 4(b). Moreover, the difference of the relative throughput between each control scheme and the simplified SCOOT scheme is enlarged compared to Scenario 1. The superiority of DETC over DATTC, which has the same triggering rate as DETC, in the queue length, the relative throughput, and the TTS demonstrates the effectiveness of the event rule proposed in this paper.

3) Scenario 3: With the increasing of the traffic demand, the TTS of the control schemes is increased significantly compared to Scenario 1 and 2 in Table I. The computational efficiency of DETC and DATTC is further demonstrated under heavy congestion by the maximum CPU time. Moreover, the relative throughput of the DETC scheme is close to that of the DATTC scheme, and the gap between the performance of the DETC scheme and the DTTC scheme is also increased in 5. As the network is heavily congested in this scenario, the triggering of the optimization in each subsystem is mainly dominated by the event condition where a minimum inter-event time is imposed, as other triggering conditions are more likely to be satisfied in the congested traffic condition. Thus the DETC scheme operates like a time-triggered scheme as the DATTC scheme.

We further investigate the traffic signals of the Yizhou-Tianlin intersection. The green time duration of the first phase for the representative intersection under the different control schemes is plotted in Fig. 6. Since the 70th

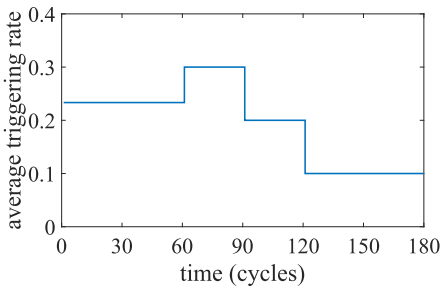

Fig. 7. Average triggering rate of the Yizhou-Tianlin intersection.

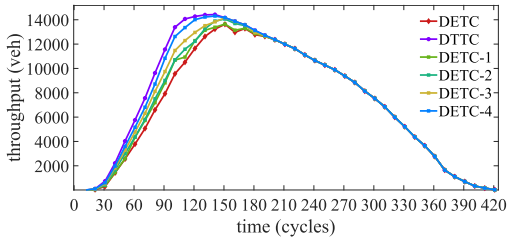

Fig. 8. The relative throughput of the modified DETC schemes.

time step, the simplified SCOOT scheme operates like a fixed-time control scheme in the saturated traffic condition, as the high traffic volume in specific phases utilizes most of the available green time, leaving less flexibility for the simplified SCOOT optimizer. In comparison, the other control schemes including the CETC, the DTTC, the DETC, and the DATTC schemes optimize the traffic signals by considering the overall performance of the system over the prediction horizon using the MPC approach, and are effective regardless of the congestion level. They operate like fixed-time controllers only after the congestion in the network is cleared. Thus they can achieve a larger performance improvement compared with the simplified SCOOT scheme in the saturated traffic condition in Scenario 2 and 3.

We also investigate the average triggering rate of the Yizhou-Tianlin intersection under DETC, which is computed every 30 cycles, as shown in Fig. 7. The average triggering rate is 0.1 after the 120th time step, implying that the update of traffic signals is triggered every 10 time steps. The long period with no changes under DETC, DATTC, and DTTC in Fig. 6 indicates that the optimization results of traffic signals for this period are the same.

To investigate the effectiveness of the DETC scheme, we have conducted an additional experiment in Scenario 3 by modifying some parameters of the triggering conditions (relaxing the original triggering conditions) of the DETC scheme. The relative throughput of the original DETC scheme denoted by "DETC", the DTTC scheme denoted by "DTTC", and the DETC schemes with modified parameters denoted by "DETC-1" to "DETC-4" are shown in Fig. 8. From DETC-1 to DETC-4, with the more frequent triggering of the optimization, the performance of the DETC scheme gets better. This shows that by modifying the parameters of the triggering conditions, we can get a close performance of the DETC scheme with that of the DTTC scheme. In the application to real traffic networks, the parameters of the DETC scheme should be properly designed by considering the physical constraints (such as the communication bandwidth of the network) and the control performance.

VI. Conclusion

We have proposed a novel distributed event-triggered MPC strategy for traffic signals in urban traffic networks. By designing the event conditions, the control signals of the system are updated only when triggered, which can avoid redundant calculation and communication. Because of the distributed architecture, the triggering mechanisms can be designed by each agent according to its own characteristics. Moreover, the asynchronous update of the traffic signals of the agents makes it more flexible and efficient than the centralized control strategies.

At each time step, the event conditions are verified by each agent based on its local information and the information transmitted from its neighbors at their last triggered time steps. The traffic signals will be updated only when the event conditions are satisfied. The triggering mechanisms in the proposed distributed event-triggered control strategy takes account of both the trend of the performance of each agent under the current control strategy and the necessary execution time of the updated traffic signals. The simulation results under different traffic demands demonstrate the effectiveness and the efficiency of the proposed event-triggered control scheme.

References

[1] P. Grandinetti, C. Canudas-de-Wit, and F. Garin, "Distributed optimal traffic lights design for large-scale urban networks," *IEEE Trans. Control Syst. Technol.*, vol. 27, no. 3, pp. 950–963, May 2019.

[2] J. Gregoire, X. Qian, E. Frazzoli, A. de La Fortelle, and T. Wongpiromsarn, "Capacity-aware backpressure traffic signal control," *IEEE Trans. Control Netw. Syst.*, vol. 2, no. 2, pp. 164–173, Jun. 2015.

[3] M. A. Khamis and W. Gomaa, "Adaptive multi-objective reinforcement learning with hybrid exploration for traffic signal control based on cooperative multi-agent framework," *Eng. Appl. Artif. Intell.*, vol. 29, pp. 134–151, Mar. 2014.

[4] Y. Bi, X. Lu, Z. Sun, D. Srinivasan, and Z. Sun, "Optimal type-2 fuzzy system for arterial traffic signal control," *IEEE Trans. Intell. Transp. Syst.*, vol. 19, no. 9, pp. 3009–3027, Sep. 2018.

[5] S. Lin, B. De Schutter, Y. Xi, and H. Hellendoorn, "Fast model predictive control for urban road networks via MILP," *IEEE Trans. Intell. Transp. Syst.*, vol. 12, no. 3, pp. 846–856, Sep. 2011.

[6] K. J. Astrom and B. M. Bernhardsson, "Comparison of Riemann and Lebesgue sampling for first order stochastic systems," in *Proc. 41st IEEE Conf. Decis. Control*, Las Vegas, NV, USA, Dec. 2002, pp. 2011–2016.

[7] A. Albert, "Comparison of event-triggered and time-triggered concepts with regard to distributed control systems," in *Proc. Embedded World*, Nüremberg, Germany, Feb. 2004, pp. 235–252.

[8] W. P. M. H. Heemels, K. H. Johansson, and P. Tabuada, "An introduction to event-triggered and self-triggered control," in *Proc. IEEE 51st IEEE Conf. Decis. Control (CDC)*, Maui, HI, USA, Dec. 2012, pp. 3270–3285.

[9] W. P. M. H. Heemels, J. H. Sandee, and P. P. J. Van Den Bosch, "Analysis of event-driven controllers for linear systems," *Int. J. Control*, vol. 81, no. 4, pp. 571–590, Apr. 2008.

[10] M. Mazo and P. Tabuada, "On event-triggered and self-triggered control over sensor/actuator networks," in *Proc. 47th IEEE Conf. Decis. Control*, Cancun, Mexico, Dec. 2008, pp. 435–440.

[11] J. Lunze and D. Lehmann, "A state-feedback approach to event-based control," *Automatica*, vol. 46, no. 1, pp. 211–215, Jan. 2010.

[12] W. P. M. H. Heemels, M. C. F. Donkers, and A. R. Teel, "Periodic event-triggered control for linear systems," *IEEE Trans. Autom. Control*, vol. 58, no. 4, pp. 847–861, Apr. 2013.

[13] K.-E. Åarzén, "A simple event-based PID controller," *IFAC Proc. Volumes*, vol. 32, no. 2, pp. 8687–8692, Jul. 1999.

[14] Y. Fan, G. Feng, Y. Wang, and C. Song, "Distributed event-triggered control of multi-agent systems with combinational measurements," *Automatica*, vol. 49, no. 2, pp. 671–675, Feb. 2013.
[15] W. P. M. H. Heemels and M. C. F. Donkers, "Model-based periodic event-triggered control for linear systems," *Automatica*, vol. 49, no. 3, pp. 698–711, Mar. 2013.
[16] A. Bemporad, M. Heemels, and M. Johansson, *Networked Control Systems*. London, U.K.: Springer, 2010, vol. 406.
[17] Q. Liu, Z. Wang, X. He, and D. H. Zhou, "A survey of event-based strategies on control and estimation," *Syst. Sci. Control Eng.*, vol. 2, no. 1, pp. 90–97, Dec. 2014.
[18] X.-M. Zhang, Q.-L. Han, and B.-L. Zhang, "An overview and deep investigation on sampled-data-based event-triggered control and filtering for networked systems," *IEEE Trans Ind. Informat.*, vol. 13, no. 1, pp. 4–16, Feb. 2017.
[19] L. Ding, Q.-L. Han, X. Ge, and X.-M. Zhang, "An overview of recent advances in event-triggered consensus of multiagent systems," *IEEE Trans. Cybern.*, vol. 48, no. 4, pp. 1110–1123, Apr. 2018.
[20] F. Dion and B. Hellinga, "A rule-based real-time traffic responsive signal control system with transit priority: Application to an isolated intersection," *Transp. Res. B, Methodol.*, vol. 36, no. 4, pp. 325–343, May 2002.
[21] A. Ferrara, S. Sacone, and S. Siri, "Event-triggered model predictive schemes for freeway traffic control," *Transp. Res. C, Emerg. Technol.*, vol. 58, pp. 554–567, Sep. 2015.
[22] R. Feng, Z. Lu, and G. Guo, "Analysis and synthesis of vehicle platooning with event-triggered communication," in *Proc. 36th Chin. Control Conf. (CCC)*, Dalina, China, Jul. 2017, pp. 9946–9951.
[23] S. Lin, B. De Schutter, Y. Xi, and H. Hellendoorn, "Efficient network-wide model-based predictive control for urban traffic networks," *Transp. Res. C, Emerg. Technol.*, vol. 24, pp. 122–140, Oct. 2012.
[24] A. Jamshidnejad, S. Lin, Y. Xi, and B. De Schutter, "Corrections to 'integrated urban traffic control for the reduction of travel delays and emissions,'" *IEEE Trans. Intell. Transp. Syst.*, vol. 20, no. 5, pp. 1978–1983, Jul. 2018.
[25] L. B. de Oliveira and E. Camponogara, "Multi-agent model predictive control of signaling split in urban traffic networks," *Transp. Res. C, Emerg. Technol.*, vol. 18, no. 1, pp. 120–139, Feb. 2010.
[26] P. J. Brockwell, R. A. Davis, and M. V. Calder, *Introduction to Time Series and Forecasting*. New York, NY, USA: Springer, 2002.
[27] G. P. Zhang, "Time series forecasting using a hybrid ARIMA and neural network model," *Neurocomputing*, vol. 50, pp. 159–175, Jan. 2003.
[28] G. E. Box, G. M. Jenkins, G. C. Reinsel, and G. M. Ljung, *Time Series Analysis, Forecasting and Control*. Hoboken, NJ, USA: Wiley, 2015.
[29] M. Behrisch, L. Bieker, J. Erdmann, and D. Krajzewicz, "SUMO–simulation of urban mobility: An overview," in *Proc. 3rd Int. Conf. Adv. Syst. Simulation*, Barcelona, Spain, Oct. 2011, pp. 63–68.
[30] P. B. Hunt, D. I. Robertson, R. D. Bretherton, and R. I. Winton, "SCOOT—A traffic responsive method of coordinating signals," Dept. Traffic Eng., Transp. Res. Lab., Crowthorne, U.K., Tech. Rep. LR 1014 Monograph, 1981.

Na Wu received the B.Sc. degree in control science and engineering from the Nanjing University of Science and Technology, Nanjing, China, in 2009. She is currently pursuing the Ph.D. degree with the Department of Automation, Shanghai Jiao Tong University, Shanghai, China.

Her works are about urban traffic congestion control and distributed control.

Dewei Li received the B.S. and Ph.D. degrees in automation from Shanghai Jiao Tong University, Shanghai, China, in 1993 and 2009, respectively.

He was a Post-Doctoral Researcher with Shanghai Jiao Tong University, from 2009 to 2010, where he is currently an Associate Professor with the Department of Automation. His research interests include model predictive control, intelligent control, and intelligent transportation systems.

Yugeng Xi (Senior Member, IEEE) received the Dr.Ing. degree in automatic control from the Technical University of Munich, Munich, Germany, in 1984.

Since then, he has been with the Department of Automation, Shanghai Jiao Tong University, Shanghai, China, where he became a Professor in 1988. He has authored or coauthored five books and more than 300 academic articles. His research interests include predictive control, large scale and complex systems, and intelligent robotic systems.

Dr. Xi is an Editor or an Associate Editor of 11 academic journals, including *Control Engineering Practice*, the *International Journal of Humanoid Robotics*, and *Acta Automatica Sinica*.

Bart de Schutter (Fellow, IEEE) received the Ph.D. degree in applied sciences from KU Leuven, Belgium, in 1996.

He is currently a Full Professor and the Head of the Department with the Delft Center for Systems and Control, Delft University of Technology, Delft, The Netherlands. His current research interests include multilevel and distributed control, control of discrete-event and hybrid systems, and intelligent transportation systems. He is also a Senior Editor of the IEEE TRANSACTIONS ON INTELLIGENT TRANSPORTATION SYSTEMS and an Associate Editor of the IEEE TRANSACTIONS ON AUTOMATIC CONTROL.